Received: 6 June 2022 | Revised: 2 August 2022 | Accepted: 17 August 2022

DOI: 10.1096/fj.202200837R

THE FASEB JOURNAL

RESEARCH ARTICLE

Cigarette smoke promotes inflammasome-independent activation of caspase-1 and -4 leading to gasdermin D cleavage in human macrophages

Marco Buscetta[1] | **Marta Cristaldi**[1] | **Maura Cimino**[1] | **Agnese La Mensa**[1,2] | **Paola Dino**[1,2] | **Fabio Bucchieri**[2] | **Francesca Rappa**[2] | **Santina Amato**[3] | **Tommaso Silvano Aronica**[3] | **Elisabetta Pace**[4] | **Alessandro Bertani**[5] | **Chiara Cipollina**[1,4]

[1]Fondazione RiMED, Palermo, Italy

[2]Department of Biomedicine, Neurosciences and Advanced Diagnostics (BiND), University of Palermo, Palermo, Italy

[3]Azienda di Rilievo Nazionale ed Alta Specializzazione Ospedali (A.R.N.A.S) "Civico Di Cristina Benfratelli", Palermo, Italy

[4]Istituto di Farmacologia Traslazionale (IFT)-CNR, Palermo, Italy

[5]IRCCS ISMETT - UPMC Italy, Palermo, Italy

Correspondence
Chiara Cipollina, Fondazione RiMED, Via Bandiera 11, Palermo 90133, Italy.
Email: ccipollina@fondazionerimed.com

Funding information
PO FESR Regione Siciliana, Grant/Award Number: G78I18000930007; Sicilian Region, Grant/Award Number: G77B17000110001

Abstract

Mechanisms and consequences of gasdermin D (GSDMD) activation in cigarette smoke (CS)-associated inflammation and lung disease are unknown. GSDMD is a downstream effector of caspase-1, -8, and -4. Upon cleavage, GSDMD generates pores into cell membranes. Different degrees of GSDMD activation are associated with a range of physiological outputs ranging from cell hyperactivation to pyroptosis. We have previously reported that in human monocyte-derived macrophages CS extract (CSE) inhibits the NLRP3 inflammasome and shifts the response to lipopolysaccharide (LPS) towards the TLR4-TRIF axis leading to activation of caspase-8, which, in turn, activates caspase-1. In the present work, we investigated whether other ASC-dependent inflammasomes could be involved in caspase activation by CSE and whether caspase activation led to GSDMD cleavage and other downstream effects. Presented results demonstrate that CSE promoted ASC-independent activation of caspase-1 leading to GSDMD cleavage and increased cell permeability, in the absence of cell death. GSDMD cleavage was strongly enhanced upon stimulation with LPS+CSE, suggesting a synergistic effect between the two stimuli. Noteworthy, CSE promoted LPS internalization leading to caspase-4 activation, thus contributing to increased GSDMD cleavage. Caspase-dependent GSDMD cleavage was associated with mitochondrial superoxide generation. Increased cleaved GSDMD was found in lung macrophages of smokers compared to ex-smokers and non-smoking controls. Our findings revealed that ASC-independent activation of caspase-1, -4, and -8 and GSDMD cleavage upon exposure to CS may contribute to macrophage dysfunction and feed the chronic inflammation observed in the smokers' lung.

Abbreviations: CS, Cigarette smoke; COPD, chronic obstructive pulmonary disease; PAMPs, pathogen-associated molecular patterns; LPS, lipopolysaccharide; NLRP, nucleotide-binding oligomerization domain, leucine-rich repeat-containing protein; GSDMD, gasdermin D; CSE, cigarette smoke extracts; hMDMs, human monocytes-derived macrophages; PMA, phorbol 12-myristate 13-acetate; PI, propidium iodide; ROS, reactive oxygen species; mROS, mitochondrial ROS.

KEYWORDS
alveolar macrophages, caspase, cigarette smoke, inflammasome, lung

1 | INTRODUCTION

Cigarette smoke (CS) is a major risk factor for chronic inflammatory airways diseases such as chronic obstructive pulmonary disease (COPD).[1] CS exposure causes oxidative stress and tissue damage leading to lung epithelial barrier dysfunction[2] and impairment of innate immune responses.[3] Alveolar macrophages from smoking subjects display altered cytokine expression profile and release, reduced expression of recognition molecules, defective phagocytosis as well as impaired activation in response to pathogen-associated molecular patterns (PAMPs) such as lipopolysaccharide (LPS).[4–6] This contributes to the increased risk of infection observed in smokers.[7] The molecular events leading to CS-associated lung diseases, such as COPD, are highly complex and still under investigation. Recent drug discovery efforts have focused on targeting inflammatory pathways, since inflammation is a major contributor to disease pathology. The identification of new therapeutic targets may help developing new and more effective drugs.[8]

Recently, inflammasomes have emerged as immune regulators potentially involved in CS-associated lung diseases.[9] However, the role of inflammasome-dependent responses in CS-associated inflammation is still under investigation. Limited and controversial data are available. Inflammasomes are multiprotein complexes composed by a receptor protein, an adaptor protein, known as ASC, and pro-caspase-1.[10,11] Several receptor proteins have been reported so far, including the nucleotide-binding oligomerization domain, leucine-rich repeat-containing protein (NLR) family members NLRP1, NLRP3, and NLRC4, the proteins absent in melanoma 2 and pyrin. Assembly and activation of the inflammasome complex promote autocatalytic cleavage of caspase-1, which, in turn, cleaves pro-interleukin (IL)-1β, pro-IL-18, and gasdermin D (GSDMD).[12] Upon cleavage, GSDMD forms pores into cell membranes, allowing the release of mature cytokines and increasing cell permeability eventually leading to a lytic pro-inflammatory form of cell death known as pyroptosis.[13] Recent evidences have shown that GSDMD can bind to mitochondrial membranes promoting mitochondrial damage and loss of membrane potential.[14–16]

We have recently reported that CS extracts (CSE) inhibited the NLRP3 inflammasome while promoting NLRP3-independent caspase-1 activation via the TLR4-TRIF-caspase-8 axis.[17] We showed that in the presence of bacterial LPS, CSE shifted the inflammatory response from TLR4-MyD88-NF-κB axis (inhibited by CSE) to TLR4-TRIF-caspase-8 enhancing caspase-1 activation and leading to an imbalanced immune response. In the present work, we tested the hypothesis that inflammasome-independent non-apoptotic activation of multiple caspases may lead to GSDMD cleavage during CS-associated inflammation. To this aim, we further explored the mechanisms leading to caspase-1 activation and investigated GSDMD cleavage and downstream effects in human monocytes-derived macrophages (hMDMs) exposed to CSE alone or in combination with the bacterial endotoxin LPS. Key findings were confirmed in a small set of distal lung tissue samples from smoking subjects and non-smoking controls.

2 | MATERIALS AND METHODS

2.1 | Reagents and antibodies

RPMI 1640 medium (ECB9006L), L-glutamine (ECB3000D), fetal bovine serum (FBS) (ECS0180L), sodium pyruvate (ECM0542D), HEPES (ECM0180D), and penicillin–streptomycin (ECB3001D) were purchased from Euroclone, Milan, Italy. Human M-CSF (130-096-492) was purchased from Miltenyi Biotec (Bergisch Gladbach, Germany). The following chemicals were obtained from Sigma-Aldrich (Missouri, USA): Phorbol 12-myristate 13-acetate (PMA, P8139), LPS from Escherichia coli 0111:B4 (L3012), LPS from Escherichia coli 0111:B4 fluorescein isothiocyanate (FITC) conjugate (F3665), Nigericin sodium salt (N7143), Z-VAD-fmk Caspase Inhibitor I (627610), and Triton X-100 (9002-93-1). Primary antibodies for western blot were as follows: ASC (sc-271 054) and actin (sc-81178) from Santa Cruz Biotechnology, Dallas, TX, USA; NLRP3 (D4D8T) was from Cell Signaling Technology (Massachusetts, USA) and full-length GSDMD (NBP2-33422) was from Novus Biological (Minnesota, USA); N-terminal GSDMD (ab215203) from Abcam (Cambridge, UK); caspase-1 (AG-20B-0048-C100) and caspase-4 (M029-3), from Adipogen (San Diego, USA) and MBL International (Massachusetts, USA), respectively. Primary antibodies were used at the following dilutions: anti-actin 1:10 000, anti-caspase-1 1:1000, anti-ASC 1:200, anti-NLRP3 1:500, anti-full-length GSDMD 1:1000, anti-cleaved GSDMD 1:3000, anti-caspase-4 1:1000. Immunofluorescence antibodies against human APC HLA-DR and full-length GSDMD were, respectively, from Miltenyi Biotec (130-111-790) and Cell Signaling Technology (96458S). The following secondary antibodies for western blot assay were purchased from LI-COR

(Lincoln, Nebraska USA): Goat Anti-Mouse IRDye 680RD (926-68070) and Donkey Anti-Rabbit IRDye 800CW (926-32213). Secondary antibodies were used at the following dilutions: 1:2000 for anti-mouse and 1:5000 for anti-rabbit. Goat Anti-Mouse IgG (Alexa Fluor® 594) (ab150116) and DAPI (ab228549) for immunofluorescence staining were purchased from Abcam. Hoechst fluorescent nucleic acid stain (33342) was obtained from ImmunoChemistry Technology, Bloomington, MN, USA. MitoSOX™ Red Mitochondrial Superoxide Indicator (M36008) and Lipofectamine 3000 Transfection Reagent (L3000-008) were purchased from Invitrogen (Waltham, MA, USA).

2.2 | Cell lines and primary cultures

Peripheral blood mononuclear cells (PBMCs) were isolated from buffy coats derived from healthy subjects and received by ARNAS "Civico, Di Cristina, Benfratelli" (Palermo, Italy) according to a Material Transfer Agreement signed on 6/11/2019.

Human macrophages were obtained by culturing PBMCs for 7 days in a complete RPMI 1640 medium supplemented with 10% FBS and 50 ng/ml of human M-CSF. The medium was replaced after 3 days of culture. The day before each experiment, monocyte-derived macrophages (hMDMs) were treated with trypsin–EDTA for 5 min, scraped, plated in complete medium without M-CSF into 96-well plates (5×10^4 cells/well), 24-well plates (35×10^4 cells/well), or 6-well plates (1.5×10^6 cells/well), and incubated at 37°C, with 5% CO_2. The human monocytic cell lines THP1 wild type (WT) (ATCC TIB-202) and THP1 ASC knockout (kindly provided by Prof. Veit Hornung, Ludwig-Maximilians-Universitat Munich, Munich, Germany[18]) were grown in a complete RPMI 1640 medium supplemented with 10% FBS and differentiated with phorbol 12-myristate 13-acetate (PMA, 5 ng/ml) for 48 h. The day of stimulation, culture medium was changed to 1% FBS or no serum (where indicated) and cells were stimulated as follows: 1 μg/ml LPS was added for 5 h, in the presence or absence of 20% CSE, which was obtained as previously described.[17] Where indicated, after 3 h of LPS priming, 10 μM nigericin was added in the culture medium for 1 h. Where indicated, the pan-caspase inhibitor z-VAD-fmk (zVAD) was added 1 h before CSE or LPS stimulation.

2.3 | Lung tissue samples

Lung tissue samples were obtained from patients undergoing surgery for lung cancer. Sampling did not interfere with the subsequent examinations of the specimens by the pathologist. The study protocol was approved by the Institutional Review Board for human studies at IRCCS ISMETT (# IRRB/19/19). Informed written consent was obtained from each patient. The patients were grouped as follows[19]: never smoking patients (non-smokers, $n = 3$); patients who had stopped smoking from more than 2 years (ex-smokers, $n = 5$); and smoker patients (>15 pack/year) (smokers, $n = 6$). Patients characteristics are reported in Table S1. Spirometry evaluation excluded the presence of COPD patients in selected groups. COPD patients were classified based on GOLD Guidelines 2019 (https://goldcopd.org/pocketguidereferences/gold-2019-pocket-guide-references/): forced expiratory volume in one second (FEV_1) < 80% of reference, FEV_1/forced vital capacity <70%, and bronchodilatation effect <12%. All subjects had negative skin tests for common aeroallergen extracts and had no history of asthma and/or allergic rhinitis. The patients were not under corticosteroid therapy (neither inhaled nor systemic) and not under antibiotics and did not have exacerbations during the month preceding the study.

2.4 | Isolation of total RNA and real-time quantitative PCR (RT-qPCR)

Isolation and purification of total RNA was performed using the RNeasy Mini Kit (Qiagen, Milan, Italy) according to the manufacturer's instructions. 1 μg of total RNA was reverse-transcribed to cDNA in a volume of 20 μl, using the iScript cDNA Synthesis kit (Bio-Rad, Hercules, CA, USA). To analyze GSDMD gene expression, quantitative PCR was carried out on Step One Plus Real-time PCR System (Applied Biosystems, Foster City, CA, USA) using specific FAM-labeled probe and primer (pre-validated TaqMan Gene expression assay for GSDMD (Hs00986739_g1), Applied Biosystems). Gene expression was normalized to GAPDH (pre-validated TaqMan Gene expression assay for GAPDH, Hs03929097_g1, Applied Biosystems) endogenous control gene. The specificity of the amplified products was determined by melting peak analysis. The relative expression of target gene was calculated using the $\Delta\Delta C_t$ method and was plotted as a relative fold-change compared to untreated cells that were chosen as the reference sample.

2.5 | Lactate dehydrogenase assay

At the indicated time, culture supernatants were transferred in a new 96-well plate and the lactate dehydrogenase (LDH) released from cells was measured using the CytoTox 96® Non-Radioactive Cytotoxicity Assay LDH Cytotoxicity Assay Kit (G1780, Promega) according to the

manufacturer's protocol. Absorbance was measured using a Tecan plate reader at wavelengths of 490 nm.

2.6 | Caspase activity assays

The extracellular activity of caspase-1 was determined using Caspase-Glo 1 homogeneous luminescent assay kit (Cat# G9951, Promega Corporation, Madison, WI), following the manufacturers' instructions.[20] The activity of caspase-4 was measured using Caspase-4 Assay kit (Cat# K126-100, BioVision, Milpitas, CA) following the manufacturers' instructions. As a positive control for caspase-4 activation, LPS (5 μg/ml) was transfected with Lipofectamine 3000 according to the manufacturer's protocol.

2.7 | Annexin V/propidium iodide assay

Annexin V-FITC Apoptosis Detection Kit (Cat# BMS500FI/300CE eBioscienceTM Dx, Bender MedSystems GmbH Vienna, Austria) was used following the manufacturers' instructions. After staining, cells were analyzed by flow cytometry using CytoFLEX (Beckman Coulter, Brea, CA).

2.8 | Intracellular LPS detection

5×10^4 cells/well were seeded in 96-well plates. Cells were incubated with LPS-FITC (1 μg/ml, 5 h) with or without CSE. As a positive control, LPS-FITC (5 μg/ml) was also transfected with Lipofectamine 3000. Cells were fixed and stained with 2 μM DAPI. Images were acquired using Operetta CLS (Perkin Elmer) with a 63× objective.

2.9 | Immunohistochemistry

For immunohistochemistry (IHC), 5-μm formalin-fixed and paraffin-embedded peripheral lung sections were deparaffinized in xylene and rehydrated through a series of graded alcohol. The sections were initially treated at 75°C in sodium citrate (pH 6.5) for antigen retrieval. After being washed, the sections were incubated with the primary antibody specific for cleaved GSDMD (36425S Cell Signaling Technologies, 1:500) at 4 °C overnight. Immunoreactivity was visualized using a Mouse and Rabbit Specific HRP/DAB Detection IHC kit (ab64264, Abcam, USA) according to the manufacturer's instructions and counterstained with Mayer's Hematoxylin for 45 s. Finally, the slides were prepared for observation with coverslips, using a permanent mounting medium (Vecta Mount, Vector, H-5000). The sections were observed with an optical microscope (Microscope Axioscope 5/7 KMAT, Carl Zeiss, Milan, Italy) connected to a digital camera (Microscopy Camera Axiocam 208 color, Carl Zeiss, Milan, Italy) for evaluation. Two independent observers (F.B. and F.R.) evaluated the reactions on two separate occasions and performed an immunomorphological evaluation to distinguish and characterized the GSDMD-positive cells. A quantitative analysis to determine the percentage of immunopositivity was also carried out. All evaluations were made at a magnification of 400× and the percentage of positive cells was calculated in a high-power field (HPF) and repeated for 10 HPFs. The arithmetic mean of counts was used for statistical analysis. All statistical analyses were performed using the program GraphPad PrismTM 9.0.1 (GraphPad Software Inc., San Diego, CA). One-way ANOVA followed by the Bonferroni post hoc test for multiple comparisons was selected as an appropriate method for data analysis. All data are presented as mean ± SEM, and the level of statistical significance was set at $p < .001$.

2.10 | Western blot

Cells were lysed using a lysis buffer made as follows: 10 mM Tris–HCl, 50 mM NaCl, 5 mM EDTA, 1% Nonidet P-40, protease inhibitor (P8340, Sigma-Aldrich, St. Louis, MO), and phosphatase inhibitor (P0044, Sigma-Aldrich, St. Louis, MO). Total protein content was determined using the Bradford protein assay kit (Thermo Fisher, Waltham, MA). A total of 60 μg protein was loaded, resolved by sodium dodecyl sulfate–polyacrylamide gel electrophoresis and blotted onto nitrocellulose membranes (Bio-Rad, Hercules, CA). For supernatant precipitation, cells were stimulated in the medium without FBS and samples were processed as previously described.[21] Blots were incubated overnight with primary antibodies at 4°C. The blots were analyzed using the Odyssey Imaging System (LI-COR, Lincoln, NE).

2.11 | ASC speck detection

ASC speck formation was assessed in hMDMs. 5×10^4 cells/well were seeded in 96-well plates, primed with LPS for 3 h, and, where indicated, with Nigericin as a positive control. After 90′, cells were fixed in paraformaldehyde/phosphate-buffered saline (PBS) 4% for 10′ at room temperature (RT), permeabilized with Triton X-100 0.2% for 5′ at RT, blocked with PBS/bovine serum albumin 3% for 30′ at RT and incubated with anti-ASC primary antibody (1:150, 1 h at RT) followed by secondary goat anti-mouse Alexa 594 antibody (1:500, 45′ at RT) and DAPI staining solution (1:5000, 10′

at RT). Image acquisition was performed using Operetta CLS (Perkin Elmer) with a 40× objective.

2.12 | Mitochondrial superoxide detection

5×10^4 cells/well were seeded in 96-well plates. After stimulation, cell medium was replaced by 1 μM MitoSOX Red + Hoechst staining (1.5 μg/ml) in PBS for 15′ at 37°C. Cells were fixed and images were acquired using Operetta CLS (Perkin Elmer) using a 40× objective.

For flow cytometry analysis, 35×10^4 cells/well were seeded in 24-well plates. After stimuli cells were harvested, washed with PBS and stained with 1 μM MitoSOX Red probe for 15′ at 37°C. Cells were washed twice in PBS and analyzed by flow cytometry using CytoFLEX (BeckmanCoulter). The results were expressed as mean fluorescence intensity.

2.13 | Statistical analysis

Statistical analysis was performed using the GraphPad Prism 9 software. Unless otherwise stated, data were expressed as mean ± SEM. Differences were identified using one-way repeated measures ANOVA with Bonferroni post hoc test. Differences with $p < .05$ were considered significant.

3 | RESULTS

3.1 | Activation of caspase-1 by CSE does not require ASC

We have recently reported that exposure of hMDMs to CSE downregulates the NLRP3 inflammasome and activates caspase-1.[17] When combined with LPS, CSE shifted the inflammatory response from TLR4-MyD88 to

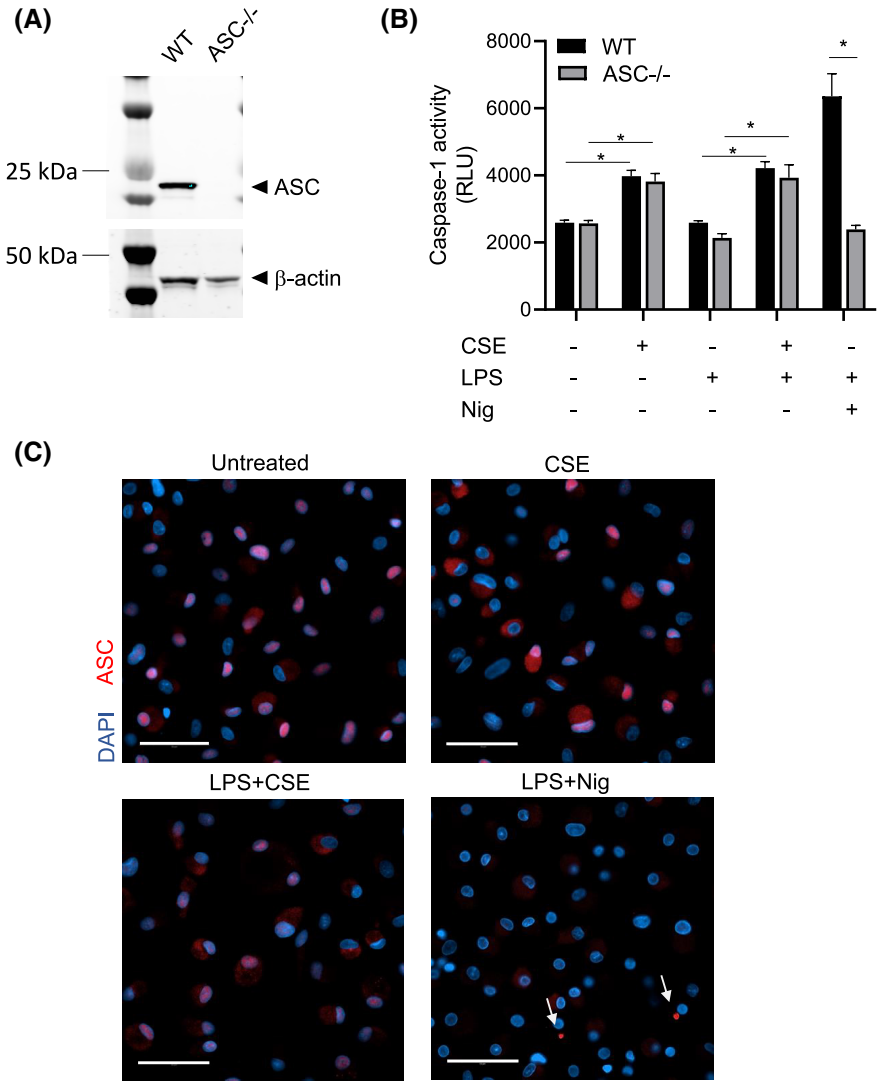

FIGURE 1 Caspase-1 activation in response to cigarette smoke extract (CSE) is independent of ASC. PMA-differentiated THP1 wild type (WT) and ASC$^{-/-}$ (A,B), and hMDMs (C), were treated with 20% CSE ± 1 μg/ml LPS. After 4 h, 10 μM nigericin (Nig) was added for 1 h. (A) Expression of ASC in THP1 WT and ASC$^{-/-}$ (representative image from three independent experiments). (B) Caspase-1 extracellular activity (expressed as relative luminescence unit, RLU) in THP1 WT and ASC$^{-/-}$ ($N = 3$ independent experiments). Mean ± SEM are reported. For statistical analysis, repeated measures ANOVA with Bonferroni post hoc test was applied. (C) Fluorescence microscopy analysis of ASC specks in hMDMs stained for ASC. Images are representative of three independent experiments/donors. Scale bar: 50 μm.

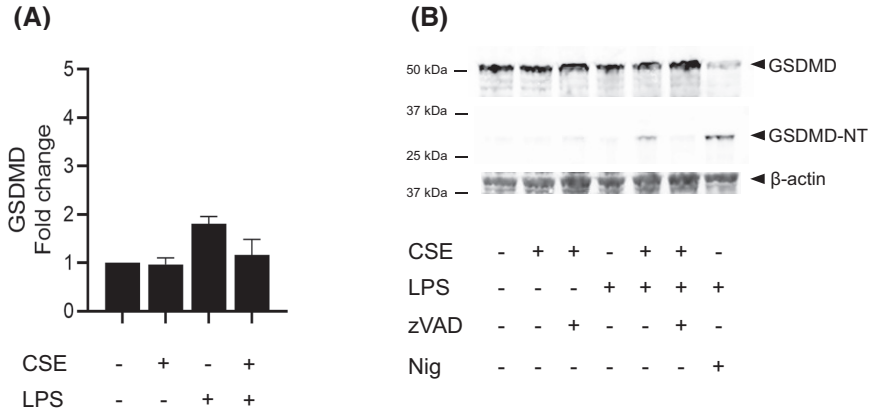

FIGURE 2 CSE promotes caspase-dependent GSDMD cleavage. hMDMs were treated with 20% CSE ± 1 μg/ml of LPS for 5 h. Where indicated, 10 μM zVAD was added 1 h before CSE/LPS. 10 μM nigericin (Nig) was added after LPS priming for 1 h. (A) GSDMD gene expression measured by RT-PCR. Values are represented as relative fold-change compared to untreated cells. Data are presented as mean ± SEM ($N = 3$ independent experiments/donors). For statistical analysis, repeated measures ANOVA with Bonferroni post hoc test was applied. (B) Western blot analysis of full-length and cleaved GSDMD expression (representative image of three independent experiments/donors).

TLR4-TRIF axis enhancing activation of caspase-8, which, in turn, cleaved and activated caspase-1.[17] Herein, we further expanded our investigation to assess whether other ASC-dependent inflammasomes could be involved in caspase-1 activation by CSE. For this purpose, we evaluated caspase-1 activation in response to CSE, alone or in combination with LPS, in THP1 macrophages $ASC^{-/-}$.[18] Results were compared with those obtained in WT cells (Figure 1A,B). Exposure of LPS-primed THP1 cells to nigericin was used as control for canonical NLRP3 inflammasome activation. As reported in Figure 1B, the increase in caspase-1 activity induced by CSE was comparable in $ASC^{-/-}$ and WT cells. On the contrary, $ASC^{-/-}$ THP1 cells failed to activate caspase-1 in response to LPS followed by nigericin (Figure 1B). Consistent with these findings, no ASC specks were detected in hMDMs CSE alone or LPS+CSE while they were detected upon stimulation with LPS and nigericin (Figure 1C).

3.2 | CSE promotes caspase-dependent cleavage of GSDMD

GSDMD is a major substrate of caspase-1.[10,11] The effects of CS exposure on GSDMD expression and cleavage in human macrophages are unknown. Both caspase-8 and caspase-1 have been reported to directly cleave GSDMD.[12] With the aim to explore the effects of CSE downstream caspase activation, we investigated GSDMD expression and cleavage in hMDMs exposed to CSE, alone or in combination with LPS. Stimulation with LPS followed by nigericin was used as a positive control for GSDMD cleavage (Figure 2B). When looking at the total levels of GSDMD (mRNA and protein), a slight increase in GSDMD mRNA was observed in response to LPS, but this did not reflect in changes at the protein level (Figures 2 and S1). Western blot analysis of cleaved GSDMD in total cell extracts revealed the formation of GSDMD-NT upon stimulation with CSE in combination with LPS but not with CSE alone (Figure 2B). To evaluate whether this was related to the limit of sensitivity of the western blot technique, we increased the amount of loaded proteins, from 60 to 100 μg, and were able to observe a band for cleaved GSDMD also in cells exposed to CSE alone (Figure S2). Treatment with the pan-caspase inhibitor z-VAD-fmk (zVAD) reverted this effect. Cleaved GSDMD localizes into cell membrane to generate pores.[12] To evaluate whether CSE promoted GSDMD localization into cell membranes, immunofluorescence analysis was performed after staining hMDMs for GSDMD using HLA-DR as marker for cell membrane. Figure 3 shows increased GSDMD and HLA co-localization on cell membranes when cells were exposed to CSE, alone or in the presence of LPS.

3.3 | CSE causes LPS internalization and activation of caspase-4

Western blot results reported in Figures 2B and S2 showed that cleavage of GSDMD was much more efficient when cells were exposed to CSE+LPS compared to CSE alone. This suggested that the presence of LPS enhanced the impact of CSE on GSDMD cleavage with unknown mechanisms. Caspase-1, -4, and -8 can cleave GSDMD after Asp275.[12] Herein, we extended our investigation to evaluate whether, in addition to caspase-1 and -8, the exposure of LPS in combination with CSE may also lead to the activation of caspase-4. For this purpose, activation of caspase-4

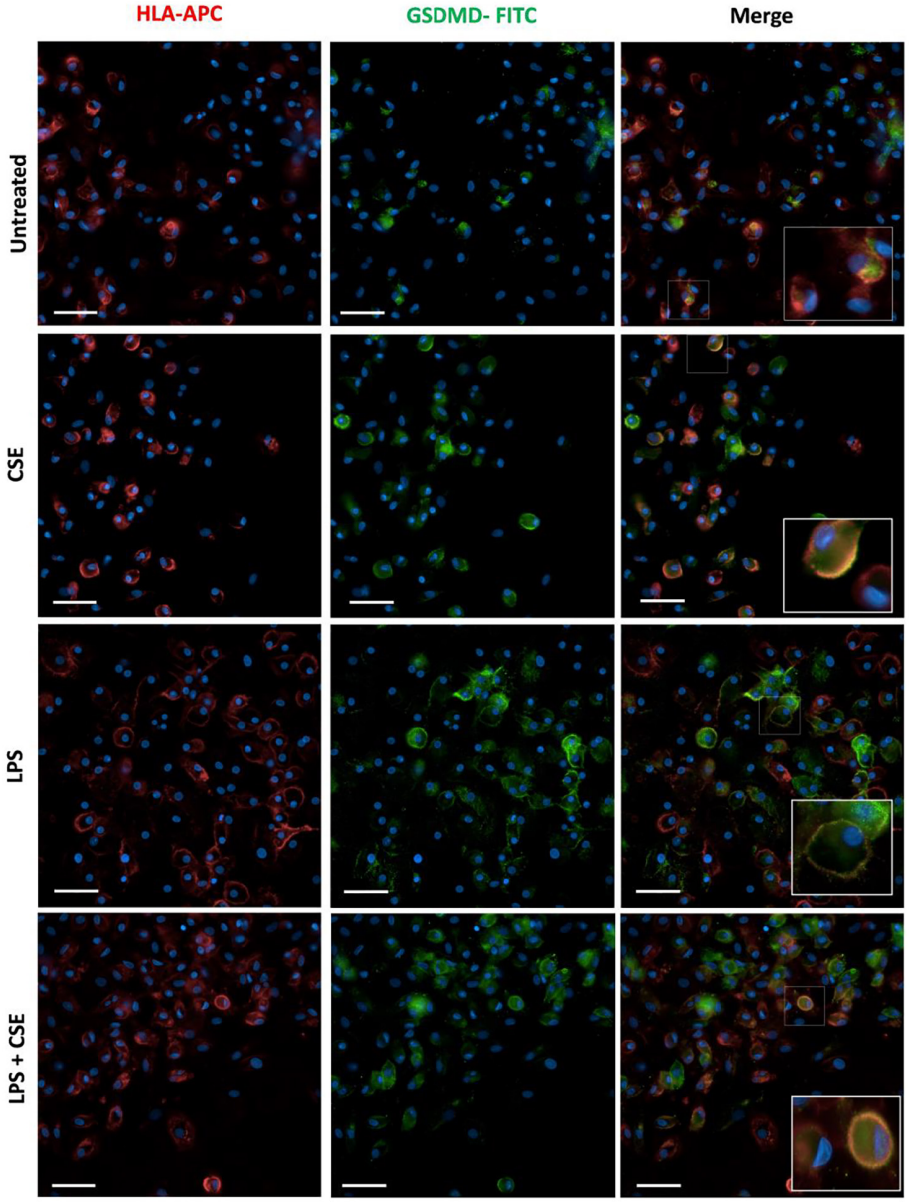

FIGURE 3 CSE promotes GSDMD localization into cell membrane. hMDMs were exposed to 20% CSE ± 1 μg/ml of LPS for 5 h. After stimulation, cells were stained with DAPI (blue), anti-human APC HLA-DR (as cell membrane marker, red) and anti-full-length GSDMD (green). Images are representative of three independent experiments/donors. Scale bar: 50 μm.

was evaluated using a fluorescent enzymatic assay. Data reported in Figure 4A show significantly increased caspase-4 activity in cell extracts of hMDMs exposed to CSE+LPS but not to LPS or CSE alone. Transfection of LPS was used as a positive control as intracellular LPS activates caspase-4 through direct binding.[22] Activation of caspase-4 in response to CSE+LPS was further confirmed by western blot analysis that showed cleaved caspase-4 in supernatant precipitates (Figure 4B). Aiming at investigating the possible mechanisms leading to caspase-4 activation, we hypothesized that CSE may promote LPS internalization. This was based on previous reports showing that cells exposed to CS display increased permeability to PAMPs, such as poly(I:C).[23] To test this hypothesis, hMDMs were treated with FITC-conjugated LPS, alone or in combination with CSE, and LPS internalization was evaluated by fluorescence imaging. Transfection of FITC-LPS was used as a positive control. Images shown in Figure 4C confirmed that CSE induced LPS internalization.

3.4 | Caspase activation by CSE increases cell permeability without leading to cell death

CSE promoted GSDMD cleavage and localization into cell membranes. We therefore tested whether this was accompanied by an increase of cell permeability. For this purpose,

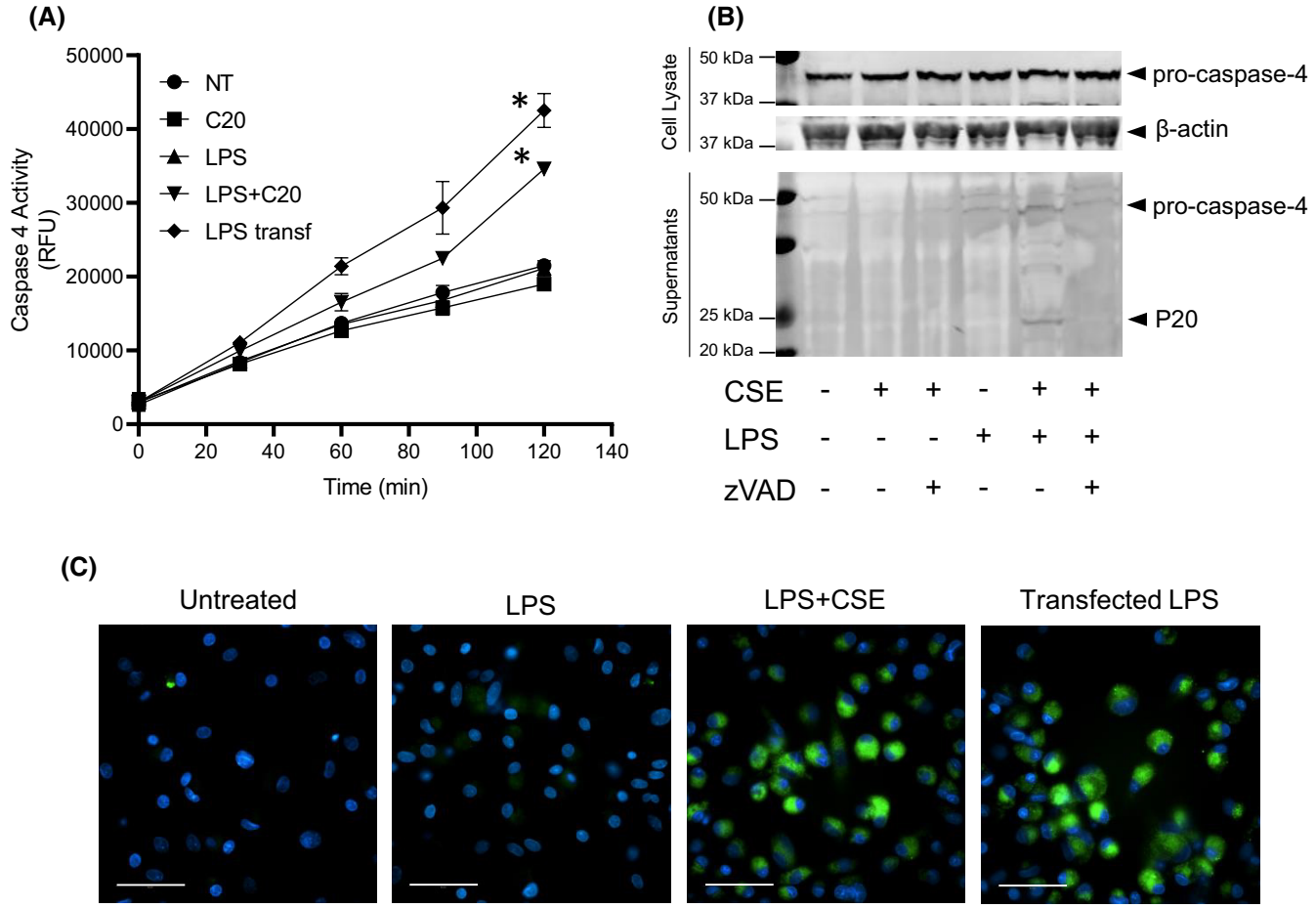

FIGURE 4 CSE promotes LPS internalization leading to caspase-4 activation. hMDMs were treated with 20% CSE ± 1 μg/ml of LPS for 5 h. (A) Time-course analysis of caspase-4 intracellular activity. Data are represented as Relative Fluorescence Unit (RFU). Mean ± SEM is reported ($N = 3$ independent experiments/donors). For statistical analysis, repeated measures ANOVA with Bonferroni post hoc test was applied. *Statistically different from LPS. (B) Western blot analysis of caspase-4 in cell lysates and supernatants (representative image from three independent experiments/donors). (C) Cells were stimulated with FITC-conjugated LPS 1 μg/ml ± 20% CSE and LPS internalization was evaluated by fluorescence microscopy. Images are representative of three independent experiments/donors. Scale bar: 50 μm.

propidium iodide (PI) internalization was evaluated by flow cytometry. CSE, alone and in combination with LPS, increased cell permeability as shown in Figure 5A. This effect was reverted by zVAD. No cell death by pyroptosis or apoptosis was observed, as measured by Annexin V/PI staining and LDH release (Figure 5B,C).

3.5 | Cleaved GSDMD is increased in lung macrophages from smokers

Data so far presented indicated that exposure of hMDMs to CSE promotes the activation of multiple caspases leading to GSDMD cleavage. We therefore hypothesized that cleaved GSDMD may be increased in lung macrophages of smoking subjects. Using an antibody specific for cleaved GSDMD (GSDMD-NT), we performed IHC analysis on distal lung tissue sections derived from three small study groups: smokers ($n = 6$), ex-smokers ($n = 5$), and non-smokers ($N = 3$). Patients characteristics are reported in Table S1. As shown in Figure 6, the percentage of lung macrophages positively stained for GSDMD-NT was significantly higher in smokers compared to ex-smokers and non-smoking controls.

3.6 | CSE leads to caspase-dependent mitochondrial damage

CS promotes oxidative damage and mitochondrial dysfunction.[24] Active caspase-1 and caspase-8[25] as well as cleaved GSDMD have been associated with mitochondrial damage.[14] Therefore, we hypothesized that CSE may promote mitochondrial damage via activation of multiple caspases and GSDMD cleavage. Mitochondrial superoxide production was measured by flow cytometry

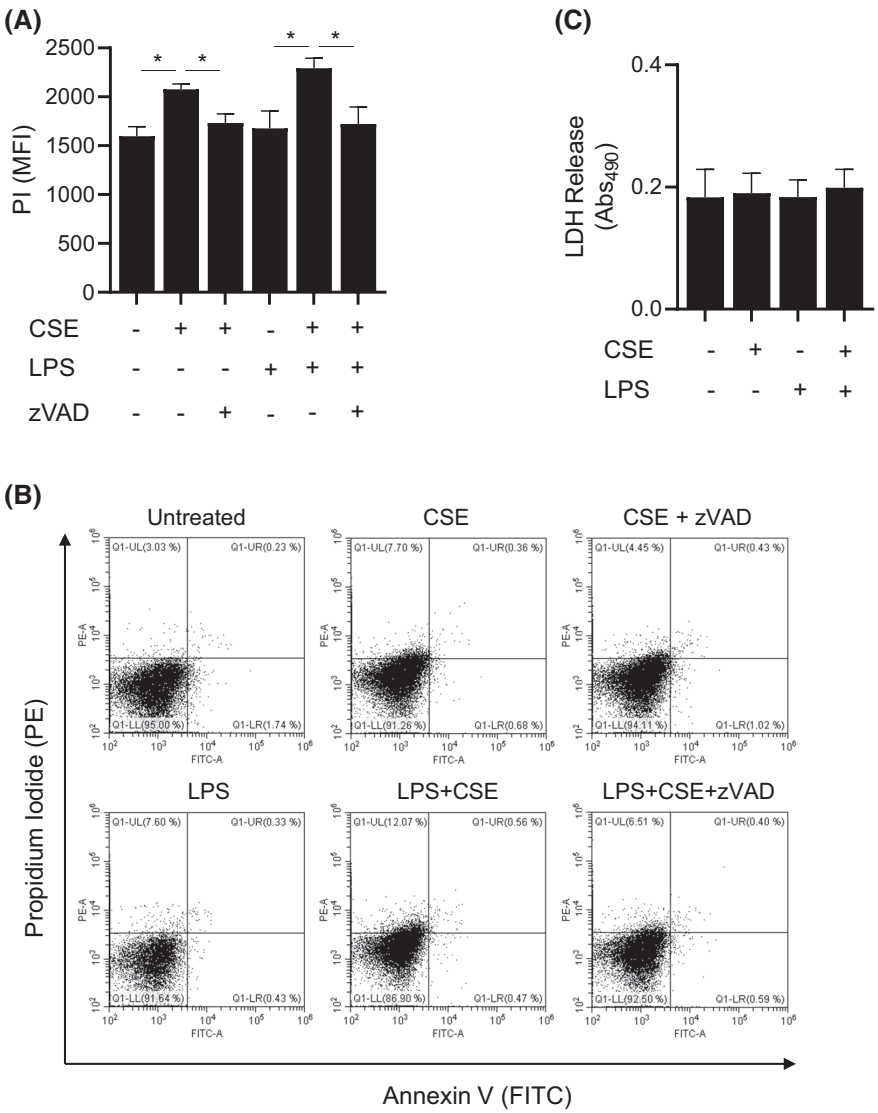

FIGURE 5 CSE increases cell permeability without inducing apoptosis or pyroptosis. hMDMs were treated with 20% CSE ± 1 μg/ml LPS for 5 h. Where indicated, 10 μM zVAD was added 1 h before LPS priming. (A) Flow cytometry analysis of PI internalization expressed as mean fluorescence intensity (MFI). (B) Representative dot plots of Annexin-V-fluorescein isothiocyanate (FITC) and PI staining. (C) Lactate dehydrogenase (LDH) release. The absorbance of LDH was measured at 490 nm. Data are presented as mean ± SEM ($N = 3$ independent experiments/donors). For statistical analysis, repeated measures ANOVA with Bonferroni post hoc test was applied.

in hMDMs exposed to CSE alone or in combination with LPS in the presence or absence of zVAD. Results reported in Figure 7 show that CSE, alone or in combination with LPS, increased mitochondrial superoxide release and that zVAD reverted this effect. Fluorescence imaging of hMDMs stained with mitochondrial superoxide indicator MitoSOX red confirmed these results (Figure 7B).

4 | DISCUSSION

Alveolar macrophages are sentinel cells strategically positioned in the alveolar space. They represent the most abundant immune cells and are the first line of defense against inhaled pathogens and particulate. Cigarette smoking suppresses key macrophage activities, such as cytokine release, surface molecule expression and phagocytosis, therefore reducing host defenses.[3] The molecular events triggered by CS are multiple and involve several signaling pathways most of which are still unknown. With regard to the impact of CS on inflammasome-dependent responses, current literature suggests that the immunosuppressive effects of CS encompass inhibition of NLRP3, IL-1β and IL-18.[5,17,26]

We have discovered that in human macrophages CSE promotes caspase-1 activation via the TLR4-TRIF-caspase-8 pathway.[17] In the presence of LPS, CSE causes profound alterations of the TLR4-dependent inflammatory responses: the TLR4-MyD88 pathway is inhibited and so is the early pro-inflammatory transcriptional program. On the contrary, activation of the TRL4-TRIF axis is enhanced leading to increased caspase-8 and caspase-1 activation.[17] Herein, we further expanded our investigation and showed that activation of caspase-1 in response to CSE occurred via ASC-independent mechanisms thus ruling out the involvement of any other ASC-dependent inflammasomes.[27] This may be a typical feature of macrophages. Inflammasome regulation by CS may follow distinct mechanisms in other lung cell types (i.e., different types of immune cells, fibroblasts and epithelial cells).

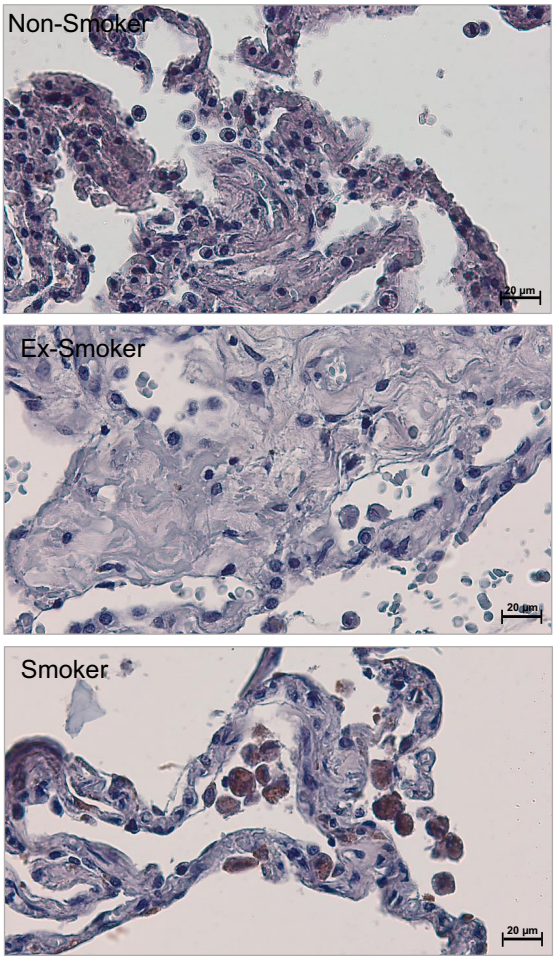

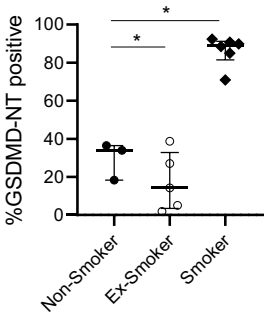

FIGURE 6 Cleaved GSDMD is increased in lung macrophages from smokers. Representative images of immunohistochemical staining of distal lung tissue sections using an antibody specific for GSDMD-NT. The graph shows the percentage of cells positive for GSDMD-NT. Data are presented as median with interquartile range. One-way ANOVA followed by the Bonferroni post hoc test for multiple comparisons was selected as an appropriate method for data analysis.

This can explain the controversial data reported regarding the NLRP3 inflammasome activation in CS-associated lung diseases.[9,28,29] On the contrary, there is wide consensus that expression and activity of caspase-1 increase in the lung of smokers and COPD subjects.[29–31] This strongly suggests that signaling pathways converging to caspase-1 activation may promote downstream effects contributing to the pathogenesis of CS-associated lung diseases, such as impaired glycolytic responses, mitochondrial damage, and altered secretory phenotype.[13,14,17]

Part of these effects may be mediated by GSDMD, a major downstream effector of caspase-1. Once cleaved by caspase-1, GSDMD-NT forms pores into cell membranes allowing unconventional secretion of IL-1 family cytokines and increasing cell permeability, eventually leading to cell death.[12] Under specific circumstances, activation of GSDMD is not associated with cell death.[32,33] Furthermore, a role for GSDMD in promoting mitochondrial damage has been reported.[13,14] Our results show that CSE, alone or in combination with LPS, promotes GSDMD cleavage and localization into cell membranes and causes caspase-dependent increase in cell permeability without leading to cell death in human macrophages. Of note, when cells were exposed to CSE in combination with the bacterial endotoxin LPS, cleavage of GSDMD was more efficient compared to stimulation with CSE alone. Caspase-1, -8, and -4 can all cleave GSDMD after Asp275.[34] We had previously reported that LPS enhanced CSE-dependent caspase-8 and caspase-1 activation.[17] Here we show that CSE promoted LPS-dependent caspase-4 activation by inducing LPS internalization, therefore highlighting an additional pathway leading to GSDMD cleavage in response to LPS and CSE. With regard to the mechanisms leading to LPS internalization in the presence of CSE, current literature suggests several hypotheses. For example, it has been reported that CSE promotes increased permeabilization to poly(I:C) upon exposure to CSE in lung epithelial cells due to enhanced caveolin-mediated endocytosis.[23] Similar mechanisms may be active in hMDMs exposed to CSE. Alternatively, LPS could be internalized via the receptor for advanced glycation endproducts (RAGE) upon binding to extracellular HMGB1, as previously reported.[35] In this respect, HMGB1 translocation and release are increased in lung macrophages exposed to CSE, and RAGE is a critical activator of alveolar macrophages in response to CS.[36,37]

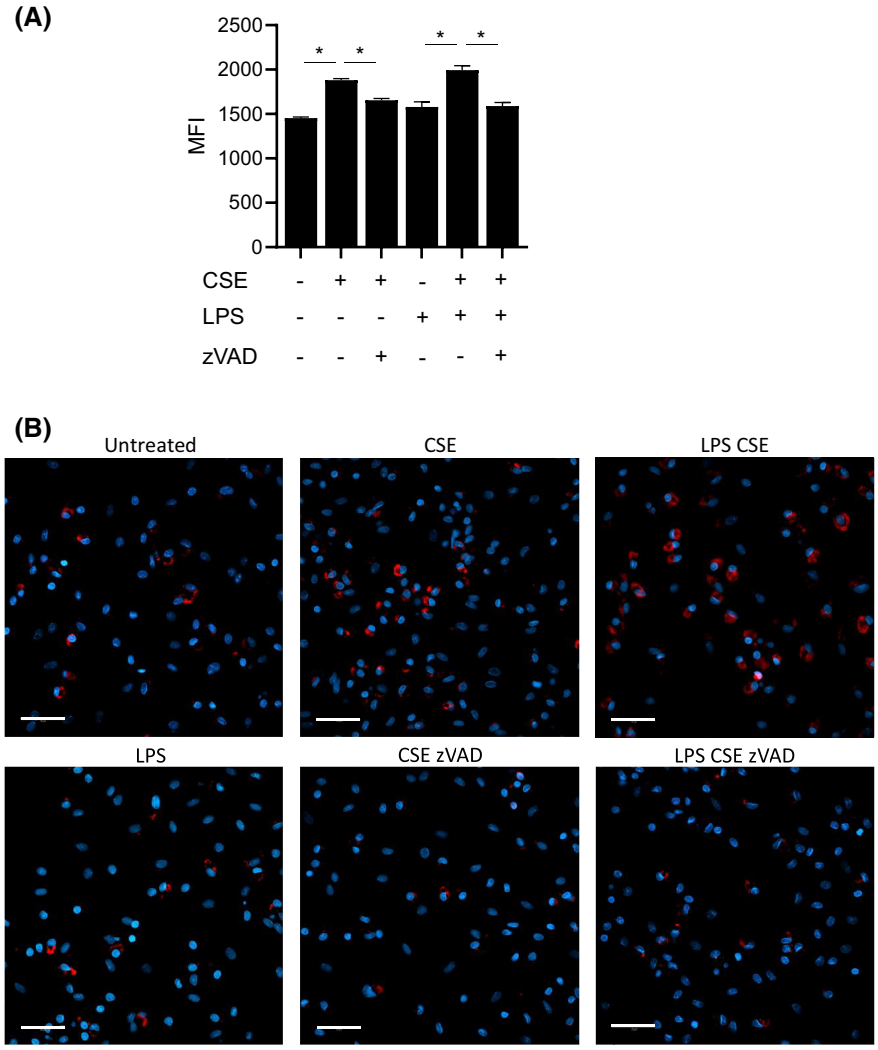

FIGURE 7 CSE induces caspase-dependent mitochondrial damage. hMDMs were treated with 20% CSE, alone or in combination with 1 μg/ml LPS for 5 h. After stimulation, cells were stained with MitoSOX red. (A) Mitochondrial superoxide detection by flow cytometry. Data are expressed as mean fluorescence intensity (MFI), with mean ± SEM of three independent experiments performed in triplicate. (B) Cells were analyzed by fluorescence microscopy. Representative images of three independent donors are shown.

Our findings clearly show that PAMPs, such as LPS, and CS can act synergistically to promote activation of caspase-1, -8, and -4 thus enhancing GSDMD cleavage (Figure 8). Whether cigarette smoking increases the accumulation of cleaved GSDMD in lung macrophages is unknown. Herein, we show that increased cleaved GSDMD is observed in lung macrophages from smokers, compared to ex-smokers or non-smoking controls. Despite the limited number of patients, these data support that cleavage of GSDMD is increased by cigarette smoking and may contribute to the pathogenesis of CS-associated lung diseases. Exposure to CS induces mitochondrial damage via multiple and partially uncovered pathways including reactive oxygen species (ROS) generation, transcriptional deregulation, and metabolic reprogramming.[38,39] Caspases and GSDMD activation have been associated with mitochondrial damage.[13,14,25] Consistently, by showing that CSE promotes the activation of caspase-1, caspase-8 and, when in combination with LPS, caspase-4, leading to GSDMD cleavage, our data reveal additional paths that may synergistically lead to mitochondrial stress generation in response to CSE alone as well as during bacterial infection. In fact, results herein reported suggest a key role for caspases in CSE-induced mitochondrial ROS (mROS) generation. This agrees with previous literature. It has been reported that caspase-1 engages multiple pathways that promote mitochondrial damage, including Parkin cleavage, mitochondrial DNA accumulation, and mROS generation.[25] Similarly, caspase-1, -4, and -8-mediated GSDMD cleavage converges toward mROS generation.[13,14]

Of note, despite leading to caspase activation, GSDMD cleavage, and mROS generation, exposure of hMDMs to CSE was not associated with cell death. In particular, we report that activation of caspase-8 after 6 h of treatment with LPS+CSE was not associated with apoptosis or pyroptosis. Treatment with zVAD reverted caspase-dependent cell permeabilization (Figure 5) and mROS generation (Figure 7). This was different compared to what had been previously reported for other experimental models where caspase inhibition by zVAD converted cell death from apoptosis to necroptosis.[40] We suggest that this may be due to the fact that

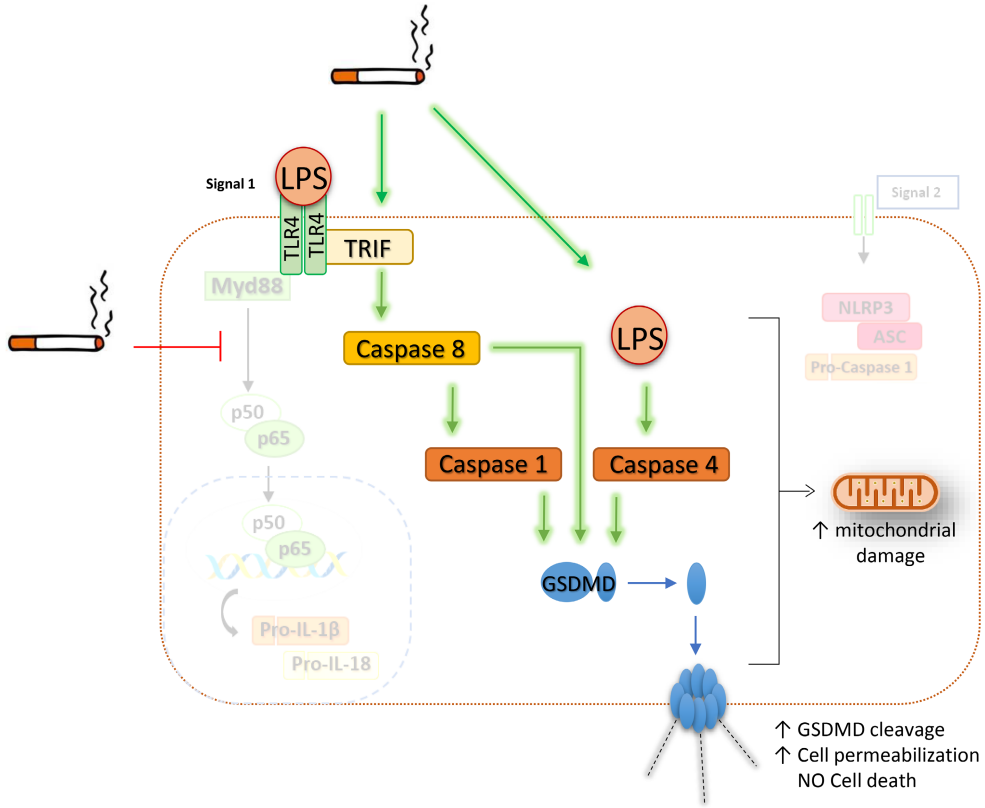

FIGURE 8 Schematic representation of the proposed model. Exposure of human macrophages to CSE activates the TRIF-caspase-8 axis leading to caspase-1 activation and GSDMD cleavage. In the presence of LPS, CSE alters the inflammatory response: the TLR4-MyD88 pathway is inhibited and so is the pro-inflammatory transcriptional program. No NLRP3 inflammasome activation occurs. Activation of caspase-8, caspase-1 and caspase-4 is promoted by CSE and LPS via multiple pathways and leads to GSDMD cleavage, increasing cell permeability with no cell death. Activation of caspases leads to mitochondrial damage.

caspase-8 activation in our experimental conditions did not reach the threshold required to induce apoptosis. Consequently, caspase inhibition by zVAD limited caspase-dependent downstream effects rather than inducing necroptosis. Overall, data herein presented are in line with growing evidence supporting an inflammatory role for cleaved caspases and GSDMD. Several reports have shown that caspase-8 displays non-apoptotic roles and participate to inflammatory reactions.[41,42] Similarly, alternative inflammasome signaling has been reported as a condition where caspase-8 and caspase-1 activation occur leading to IL-1β release from living monocytes.[43] Zanoni and colleagues have shown that hyperactivated phagocytes are characterized by caspase-11 activation by endogenous ligands leading to GSDMD cleavage with consequent release of IL-1β in the absence of cell death.[33] Evavold and colleagues have reported that GSDMD has a non-pyroptotic role allowing secretion of inflammatory mediators from living cells.[32] Overall, these data suggest that under specific circumstances, caspase activation and GSDMD cleavage may occur in living cells where they play a key role in modulating inflammatory responses. In line with these findings, our data (Figure 2B) show that the extent of GSDMD cleavage in cell stimulated with LPS in combination with CSE was much lower compared to cells stimulated with nigericin, clearly demonstrating that GSDMD cleavage can occur at a very different extent depending on the trigger. This would eventually lead to different cell fates. Specifically, we propose that the levels of active caspases and cleaved GSDMD present in hMDMs exposed to CS are low but prolonged in time.[44] This may contribute to perpetuate the accumulation of dysfunctional macrophages in smokers' lung. Accordingly, around 90% of lung macrophages from smokers positively stained for cleaved GSDMD. Of note, despite leading to caspase activation and GSDMD cleavage, treatment with LPS+CSE did not induce the release of mature IL-1β and IL-18. This was due to the previously reported inhibitory effect of CSE on LPS-induced expression of pro-IL-1β and pro-IL-18.[17]

Overall, data herein presented shed new light on the molecular mechanisms underlying macrophage dysfunction in smokers. We reveal that CS induces ASC-independent caspase activation and GSDMD cleavage contributing to altered cell permeability and mitochondrial damage. When combined with LPS, CS promoted

LPS internalization leading to caspase-4 activation further enhancing GSDMD cleavage (Figure 8). The finding that cleaved GSDMD was increased in the smoker's lung supports that these mechanisms may be of pathophysiological relevance for CS-associated lung diseases. Overall, data herein presented combined with the previously reported suppression of the TLR4-MyD88 pathway by CS[5,6,17] provide a possible explanation for the increased susceptibility to infection and the presence of chronic and unresolved inflammation in the smokers' lung.

AUTHOR CONTRIBUTIONS

Marco Buscetta, Marta Cristaldi, and Chiara Cipollina drafted the manuscript and designed the experiments. Marco Buscetta, Marta Cristaldi, Maura Cimino, Agnese La Mensa, and Paola Dino performed the experiments. Marco Buscetta, Marta Cristaldi, Maura Cimino, Chiara Cipollina, Francesca Rappa, and Fabio Bucchieri performed the data analysis. Santina Amato, Tommaso Silvano Aronica, and Alessandro Bertani provided the human samples. Marco Buscetta, Marta Cristaldi, Chiara Cipollina, and Elisabetta Pace reviewed the manuscript. All authors have read, reviewed, and approved the final manuscript.

ACKNOWLEDGMENTS

We thank Prof. Veit Hornung for providing ASC$^{-/-}$ THP1 cells and Rossella Alduino for her precious support for the clinical study submission. This work was supported by the Sicilian Region under the Programme Cohesion Development Fund 2014/2020—Grant "Patto per il Sud"—Project CheMiST—CUP G77B17000110001, by Progetto "SeNSO" to CC-CUP G78I18000930007 funded within P.O. FESR Regione Siciliana 2014/2020-Azione 1.1.5. and by Fondazione Ri. MED.

DISCLOSURES

The authors declare no conflicts of interest.

DATA AVAILABILITY STATEMENT

Data sharing not applicable to this article as no datasets were generated or analyzed during the current study.

REFERENCES

1. Barnes PJ, Burney PG, Silverman EK, et al. Chronic obstructive pulmonary disease. *Nat Rev Dis Primers*. 2015;1:15076.
2. Aghapour M, Raee P, Moghaddam SJ, Hiemstra PS, Heijink IH. Airway epithelial barrier dysfunction in chronic obstructive pulmonary disease: role of cigarette smoke exposure. *Am J Respir Cell Mol Biol*. 2018;58:157-169.
3. Lugg ST, Scott A, Parekh D, Naidu B, Thickett DR. Cigarette smoke exposure and alveolar macrophages: mechanisms for lung disease. *Thorax*. 2021;77:94-101.
4. Shaykhiev R, Krause A, Salit J, et al. Smoking-dependent reprogramming of alveolar macrophage polarization: implication for pathogenesis of chronic obstructive pulmonary disease. *J Immunol*. 2009;183:2867-2883.
5. Birrell MA, Wong S, Catley MC, Belvisi MG. Impact of tobacco-smoke on key signaling pathways in the innate immune response in lung macrophages. *J Cell Physiol*. 2008;214:27-37.
6. Hodge S, Hodge G, Ahern J, Jersmann H, Holmes M, Reynolds PN. Smoking alters alveolar macrophage recognition and phagocytic ability: implications in chronic obstructive pulmonary disease. *Am J Respir Cell Mol Biol*. 2007;37:748-755.
7. Jiang C, Chen Q, Xie M. Smoking increases the risk of infectious diseases: a narrative review. *Tob Induc Dis*. 2020;18:60.
8. Nguyen JMK, Robinson DN, Sidhaye VK. Why new biology must be uncovered to advance therapeutic strategies for chronic obstructive pulmonary disease. *Am J Physiol Lung Cell Mol Physiol*. 2021;320:L1-L11.
9. Ma Y, Long Y, Chen Y. Roles of inflammasome in cigarette smoke-related diseases and physiopathological disorders: mechanisms and therapeutic opportunities. *Front Immunol*. 2021;12:720049.
10. Broz P, Dixit VM. Inflammasomes: mechanism of assembly, regulation and signalling. *Nat Rev Immunol*. 2016;16:407-420.
11. Pinkerton JW, Kim RY, Robertson AAB, et al. Inflammasomes in the lung. *Mol Immunol*. 2017;86:44-55.
12. Lieberman J, Wu H, Kagan JC. Gasdermin D activity in inflammation and host defense. *Sci Immunol*. 2019;4:eaav1447.
13. de Vasconcelos NM, Van Opdenbosch N, Van Gorp H, Parthoens E, Lamkanfi M. Single-cell analysis of pyroptosis dynamics reveals conserved GSDMD-mediated subcellular events that precede plasma membrane rupture. *Cell Death Differ*. 2019;26:146-161.
14. Platnich JM, Chung H, Lau A, et al. Shiga toxin/lipopolysaccharide activates caspase-4 and gasdermin D to trigger mitochondrial reactive oxygen species upstream of the NLRP3 inflammasome. *Cell Rep*. 2018;25:1525-1536.e1527.
15. Rogers C, Erkes DA, Nardone A, Aplin AE, Fernandes-Alnemri T, Alnemri ES. Gasdermin pores permeabilize mitochondria to augment caspase-3 activation during apoptosis and inflammasome activation. *Nat Commun*. 2019;10:1689.
16. de Torre-Minguela C, Gomez AI, Couillin I, Pelegrin P. Gasdermins mediate cellular release of mitochondrial DNA during pyroptosis and apoptosis. *FASEB J*. 2021;35:e21757.
17. Buscetta M, Di Vincenzo S, Miele M, Badami E, Pace E, Cipollina C. Cigarette smoke inhibits the NLRP3 inflammasome and leads to caspase-1 activation via the TLR4-TRIF-caspase-8 axis in human macrophages. *FASEB J*. 2020;34:1819-1832.
18. Schmid-Burgk JL, Gaidt MM, Schmidt T, Ebert TS, Bartok E, Hornung V. Caspase-4 mediates non-canonical activation of the NLRP3 inflammasome in human myeloid cells. *Eur J Immunol*. 2015;45:2911-2917.
19. Pace E, Ferraro M, Minervini MI, et al. Beta defensin-2 is reduced in central but not in distal airways of smoker COPD patients. *PLoS ONE*. 2012;7:e33601.
20. O'Brien M, Moehring D, Munoz-Planillo R, et al. A bioluminescent caspase-1 activity assay rapidly monitors inflammasome activation in cells. *J Immunol Methods*. 2017;447:1-13.
21. Cipollina C, Di Vincenzo S, Siena L, Di Sano C, Gjomarkaj M, Pace E. 17-oxo-DHA displays additive anti-inflammatory effects with fluticasone propionate and inhibits the NLRP3 inflammasome. *Sci Rep*. 2016;6:37625.

22. Shi J, Zhao Y, Wang Y, et al. Inflammatory caspases are innate immune receptors for intracellular LPS. *Nature*. 2014;514:187-192.
23. Duffney PF, Embong AK, McGuire CC, Thatcher TH, Phipps RP, Sime PJ. Cigarette smoke increases susceptibility to infection in lung epithelial cells by upregulating caveolin-dependent endocytosis. *PLoS ONE*. 2020;15:e0232102.
24. Pourahmad J, Aghvami M, Zarei MH, Naserzadeh P. Cigarette smoke and mitochondrial damage. In: Will Y, Dykens JA, eds. *Mitochondrial Dysfunction Caused by Drugs and Environmental Toxicants*. John Wiley & Sons; 2018:709-725.
25. Yu J, Nagasu H, Murakami T, et al. Inflammasome activation leads to caspase-1-dependent mitochondrial damage and block of mitophagy. *Proc Natl Acad Sci U S A*. 2014;111:15514-15519.
26. Han S, Jerome JA, Gregory AD, Mallampalli RK. Cigarette smoke destabilizes NLRP3 protein by promoting its ubiquitination. *Respir Res*. 2017;18:2.
27. Philip NH, Dillon CP, Snyder AG, et al. Caspase-8 mediates caspase-1 processing and innate immune defense in response to bacterial blockade of NF-kappaB and MAPK signaling. *Proc Natl Acad Sci U S A*. 2014;111:7385-7390.
28. Di Stefano A, Caramori G, Barczyk A, et al. Innate immunity but not NLRP3 inflammasome activation correlates with severity of stable COPD. *Thorax*. 2014;69:516-524.
29. Markelic I, Hlapcic I, Ceri A, et al. Activation of NLRP3 inflammasome in stable chronic obstructive pulmonary disease. *Sci Rep*. 2022;12:7544.
30. Kelesidis T, Zhang Y, Tran E, Sosa G, Middlekauff HR. Expression of key inflammatory proteins is increased in immune cells from tobacco cigarette smokers but not electronic cigarette vapers: implications for atherosclerosis. *J Am Heart Assoc*. 2021;10:e019324.
31. Li C, Zhihong H, Wenlong L, et al. The nucleotide-binding oligomerization domain-like receptor family pyrin domain-containing 3 inflammasome regulates bronchial epithelial cell injury and proapoptosis after exposure to biomass fuel smoke. *Am J Respir Cell Mol Biol*. 2016;55:815-824.
32. Evavold CL, Ruan J, Tan Y, Xia S, Wu H, Kagan JC. The pore-forming protein gasdermin D regulates Interleukin-1 secretion from living macrophages. *Immunity*. 2018;48:35-44.e36.
33. Zanoni I, Tan Y, Di Gioia M, et al. An endogenous caspase-11 ligand elicits interleukin-1 release from living dendritic cells. *Science*. 2016;352:1232-1236.
34. Sarhan J, Liu BC, Muendlein HI, et al. Caspase-8 induces cleavage of gasdermin D to elicit pyroptosis during Yersinia infection. *Proc Natl Acad Sci U S A*. 2018;115:E10888-E10897.
35. Yang H, Wang H, Andersson U. Targeting inflammation driven by HMGB1. *Front Immunol*. 2020;11:484.
36. Le Y, Wang Y, Zhou L, et al. Cigarette smoke-induced HMGB1 translocation and release contribute to migration and NF-kappaB activation through inducing autophagy in lung macrophages. *J Cell Mol Med*. 2020;24:1319-1331.
37. Sanders KA, Delker DA, Hueckstead T, et al. RAGE is a critical mediator of pulmonary oxidative stress, alveolar macrophage activation and emphysema in response to cigarette smoke. *Sci Rep*. 2019;9:231.
38. Ballweg K, Mutze K, Konigshoff M, Eickelberg O, Meiners S. Cigarette smoke extract affects mitochondrial function in alveolar epithelial cells. *Am J Physiol Lung Cell Mol Physiol*. 2014;307:L895-L907.
39. Hoffmann RF, Zarrintan S, Brandenburg SM, et al. Prolonged cigarette smoke exposure alters mitochondrial structure and function in airway epithelial cells. *Respir Res*. 2013;14:97.
40. Ma Y, Temkin V, Liu H, Pope RM. NF-kappaB protects macrophages from lipopolysaccharide-induced cell death: the role of caspase 8 and receptor-interacting protein. *J Biol Chem*. 2005;280:41827-41834.
41. Burguillos MA, Deierborg T, Kavanagh E, et al. Caspase signalling controls microglia activation and neurotoxicity. *Nature*. 2011;472:319-324.
42. Orning P, Lien E. Multiple roles of caspase-8 in cell death, inflammation, and innate immunity. *J Leukoc Biol*. 2021;109:121-141.
43. Gaidt MM, Ebert TS, Chauhan D, et al. Human monocytes engage an alternative inflammasome pathway. *Immunity*. 2016;44:833-846.
44. Chan AH, Schroder K. Inflammasome signaling and regulation of interleukin-1 family cytokines. *J Exp Med*. 2020;217:e20190314.

SUPPORTING INFORMATION

Additional supporting information can be found online in the Supporting Information section at the end of this article.

How to cite this article: Buscetta M, Cristaldi M, Cimino M, et al. Cigarette smoke promotes inflammasome-independent activation of caspase-1 and -4 leading to gasdermin D cleavage in human macrophages. *The FASEB Journal*. 2022;36:e22525. doi: 10.1096/fj.202200837R